

Design of Compact Low Pass Filter with Large Reject Band Using Open Circuit Stubs and Two Cascaded DGS-Quasi- Triangular Resonators

M. Challal^{1,3}, A. Boutejdar², A. Azrar³ and D. Vanhoenacker-Janvier¹

¹ ICTEAM, UCLouvain, Bâtiment Maxwell, 3 place du Levant, B-1348 Louvain-la-Neuve, Belgium
{mouloud.challal, danielle.vanhoenacker}@uclouvain.be

² Chair of Microwave and Communication Engineering, University of Magdeburg, Magdeburg, 39106,
Germany
Ahmed.Boutejdar@ovgu.de

³ Department of Electronic, IGEE, University of Boumerdes, Av. de l'indépendance, B-35000
Boumerdes, Algeria
{mchallal, a_azrar}@umbb.dz

Abstract—This paper investigates a quasi triangular of defected ground structure (DGS) for low-pass filters (LPFs) application. An equivalent *RLC* circuit model is presented and its corresponding parameters are as well extracted using the parametric relationships. The LPFs using the proposed DGS pattern combined with open stubs are designed and fabricated. The proposed LPF presents the advantages of small size, low insertion loss and ultra-wide stopband with 20 dB attenuation from 4 GHz to more than 20 GHz. The simulated results obtained by equivalent circuit model (ECM) and full-wave EM show good agreement with the measured ones.

I. INTRODUCTION

Recently, there has been an increasing interest in microwave circuits design especially microstrip filter using defected ground structure (DGS). Nowadays, many researchers focus on this type of structure because it offers various advantages such as well applied to RF/microwave circuits to reduce the size [1]-[5], improve the performances [6]-[9] and easily performed to extract the equivalent circuit [1]-[4].

A DGS is realized by etching off a defected pattern from the ground plane. An etched defect disturbs the shield current distribution in the ground plane. This disturbance changes the characteristics of the transmission line to achieve the slow-wave effect and bandstop property [1]-[3]. It provides an attenuation pole frequency (f_0) and a cutoff frequency (f_c). A variety of DGS shapes for low-pass filters (LPF) applications has been presented in literature such as dumbbell shaped DGS [1]-[3], semicircle shaped DGS [4], elliptic shaped DGS [10], asymmetric DGS [11], cross-shaped DGS [12], equilateral u-shaped DGS [13], dual reverse U-shaped DGS [14], multiple T-shaped DGS [15]. However, there is always a tradeoff between the performance (such as stopband and passband characteristics) and the physical size of the filter.

In this work, a quasi triangular of DGS is proposed for LPF design, which is simple, compact and has controllable topology. The use of the proposed DGS pattern along with H shape open stubs [10] provides a wider and deeper stopband and compact in size than the conventional LPFs [12]-[15]. The analysis of different number of DGS-LPF is investigated and carried out with the EM simulation IE3D software. Equivalent circuit model (ECM) based on lumped elements (*LCR* parallel resonant circuit) [10] is used to characterize the proposed DGS-LPF. Its frequency response is obtained using the Agilent ADS circuit simulator. The substrate material used for the design is RO4350B Rogers material with a thickness of 0.254 mm and a relative permittivity of 3.63. The conductor strip of the microstrip line (50Ω) on the top plane has a calculated width w of 0.52 mm. The theoretical and measured results are presented with good agreement for LPF fabrication.

II. DESIGN CONCEPT AND CIRCUIT MODELING

The proposed DGS pattern is obtained by etching a slot connecting with two half of modified triangular defected in the ground plane, as Figure 1 shown. Similarly to the conventional structures [1]-[3], this structure provides an attenuation pole frequency f_0 and a cutoff frequency f_c . Therefore, it can be

represented by a *LCR* parallel resonance circuit in series with the transmission line [10] as shown in Figure 1.

The proposed DGS dimensions ℓ_1, ℓ_2, g and c are considered to be respectively 7.14, 4.84, 0.5 and 0.94 mm and the circuit elements are extracted using the following equations [10].

$$C = \frac{\omega_0}{2Z_0(\omega_0^2 - \omega_c^2)} \quad (1)$$

$$L = \frac{1}{\omega_0^2 C} \quad (2)$$

$$R = \frac{2Z_0}{\sqrt{\frac{1}{|S_{11}(\omega_0)|^2} - (2Z_0(\omega_0 C - \frac{1}{\omega_0 L}))^2 - 1}} \quad (3)$$

where $\omega_0 = 2\pi f_0$ and $\omega_c = 2\pi f_c$ are the angular resonance frequency and 3-dB cutoff frequency of the DGS, respectively.

To confirm the validity of the ECM, a comparison on S-parameters with the full-wave electromagnetic (EM) simulations is presented in Figure 2. The extracted elements L, C and R are respectively 2.73 nH, 0.32 pF and 2.31 k Ω . Good agreement for both insertion and return losses can be seen whereas some discrepancies appear for frequencies higher than f_0 . It could be caused by the simplicity of the equivalent lumped model; the distributed effects are not included.

III. DETERMINATION OF AN APPROACH EQUIVALENT CIRCUIT USING THE DISTRIBUTION OF EM-FIELD ALONG OF THE PROPOSED DGS-RESONATOR

The objective of this short investigation is to verify the dependence of the equivalent circuit elements on the surface as the distribution of electromagnetic field. The field simulation results are shown in Figure 3 (a-b). As Figure 3.a shows, at the frequency $f = 1$ GHz the RF power is transmitted from input port to output port. At the reject frequency $f = 5.5$ GHz the signal is blocked in port one as shown in Figure 3.b. As known, at resonance frequency, the field is concentrated along the DGS-unit as two

equal electric and magnetic energies. The magnetic field is located around the triangular area (zone I) while the electric field is concentrated in a small channel slot (zone II) as shown in Figure 3. Depending on this field method, the EM distribution leads to design an approach equivalent circuit that corresponds to the DGS-resonator, thus to design an approximated circuit of the desired filter.

IV. EFFECT OF THE DGS DIMENSIONS ON THE PERFORMANCES

For the proposed DGS, the effect of the dimensions, the physical lengths ℓ_1, ℓ_2 , c and the width g on the performance of the resonator are studied, based on EM simulation results. The structure shown in Figure 1 with $\ell_1 = 7.14$ mm, $\ell_2 = 4.84$ mm, $g = 0.5$ mm and $c = 0.94$ mm is used in this study.

Figure 4 shows both the magnitudes of the transfer function (S_{21}) and the input reflection coefficient (S_{11}) when ℓ_1 is varied while the other parameters of the structure are kept constant. The obtained characteristics of the proposed DGS pattern are summarized in Tables 1. From the data in Table 1, it can be seen that an increase in ℓ_1 , leads to a decrease in attenuation pole frequency (f_0), cutoff frequency (f_c) and stopband width (BW_{20dB}) whereas S_{21max} slowly increases with increasing of the length ℓ_1 . Besides, the capacitance, inductance and resistance extracted by using (1), (2) and (3), respectively, increase with the increase of the length ℓ_1 .

The characteristics of the proposed DGS pattern with different ℓ_2 , c and g are also summarized in Tables 2, Table 3 and table 4, respectively. It is observed from Table 2 that f_0, f_c and BW_{20dB} decrease when ℓ_2 increases whereas S_{21max} increases with increasing ℓ_2 . In addition, the capacitance and inductance increase with the increase of the length ℓ_2 . A rapid increase on the resistance is observed when increasing the length ℓ_2 . From Table 3, it is observed that an increase in c , leads to a decrease in both f_0 and f_c while S_{21max} slowly decreases. Moreover, the capacitance and the inductance increase with the increase of the length c whereas the resistance progressively decreases with increasing the length c . From Table 4, it can be seen that f_c do not change with the width g whereas f_0 and BW_{20dB}

increase and S_{21max} decreases with increasing g . Furthermore, the inductance and resistance increase with the increase of the width g whereas the capacitance gradually decreases with increasing the width g . Therefore, a proposed DGS operating at different selected attenuation pole frequency can be designed by simply varying the width g .

V. PROPOSED DGS BASED LOW-PASS FILTER: DESIGN CONCEPT AND CIRCUIT MODELING

The proposed structure of the DGS-LPF is shown in Figure 5. The filter consists of a proposed shaped DGS along with two open stubs known as H shape open stubs [10]. The use of H open stubs in the proposed DGS pattern permits to increase the coupling capacitance between 50Ω microstrip line and proposed DGS pattern. Therefore, the characteristics of the proposed DGS-LPF are dependent on the dimensions of both DGS pattern and open stubs. The physical parameters of this DGS-LPF structure, $\ell_1 = 8.14$ mm, $\ell_2 = 5.5$ mm, $c = 0.24$ mm, $g = 1$, $L_s = 6$ mm and $W_s = 1.3$ mm, are considered.

Based on the above discussion, the proposed DGS-LPF can be modeled as one resonator along with two shunt capacitors C_p which correspond to the open stubs as shown in Figure 5.

According to the basic theories of transmission lines, an open stub is modeled as an equivalent capacitor. The equivalent capacitance with the characteristic impedance (Z_s) and length (ℓ_s) can be obtained from [16] as:

$$C_p = \frac{1}{\omega Z_s} \tan\left(\frac{2\pi\ell_s}{\lambda_g}\right) \quad (4)$$

where λ_g represents the guided wavelength.

The elements L_1 , C_1 and R_1 of Figure 5 are extracted by the equations described by (1), (2) and (3) and their values are respectively 4.70 nH, 3.89 pF and 3.50 k Ω whereas the shunt capacitance C_p obtained by the equation (4) is 1.09 pF.

The EM and circuit model simulation results of the proposed DGS-LPF are shown in Figure 6. The 3-dB cutoff frequency of the proposed filter is equal to 3.1 GHz.

From the data provided in Figure 6, it is observed that the insertion loss is equal to 0.10 dB and the return loss is better than 26 dB in the whole passband. Moreover, a wide suppression band at attenuation level of -20 dB starting from 6 GHz to more than 20 GHz is achieved in the stopband.

From Figure 6, reasonably good agreement between circuit model and full-wave EM simulations for insertion loss can be seen below 8 GHz, whereas some discrepancies appear at a higher than 8 GHz. For return loss, good agreement can be seen above 1.5 GHz whereas some difference appears from 0.2 to 1.5 GHz. It could be resulted from the simplicity of the lumped circuit model that the distributed effects are not included in this model. This result shows that the circuit model provides quite good performances and confirms its validity.

To further improve the stopband rejection, filter based on more than one DGS pattern should be used. Figure 7 (a-b) shows the geometry and the circuit model of the proposed LPF using two cascaded DGS patterns and three open stubs. By using equation (4), the shunt capacitance C_p is equal to 2.07 pF. The width W_{S1} of the open stub is selected to 2 mm.

Figure 8 shows a comparison of S -parameters between a filter with 01 DGS pattern along with two open stubs and a filter with 02 DGS patterns along with 03 open stubs. From Figure 8, one can realize that by increasing the number of DGS pattern, the proposed DGS-LPF achieves return loss throughout passband range above 20 dB whereas in the stopband is more than 20 dB at an ultra-wide range from 4 GHz to more than 20 GHz. In addition, low insertion loss in the passband and sharp response in transition domain are obtained due to the open stubs and the resonance characteristic of two-cascaded DGS patterns.

Comparison of the insertion and return losses between the results by the full-wave EM simulation and the extracted lumped model is shown in Figure 9. It can be seen from Figure 9 that the circuit model provides good performances and confirms its validity in certain band of frequencies.

VI. IMPLEMENTATION AND MEASUREMENT

The proposed LPF with one DGS in the metallic ground plane and two open stubs on the top layer is fabricated as shown in Figure 10; whereas, the measured and simulated results are shown in Figure. 11. From the measured results shown in Figure 11, it can be seen that the fabricated LPF has a 3-dB cutoff frequency at 3.1 GHz, the insertion loss is as low as 0.1 dB in the passband of the LPF and stopband is suppressed below -20 dB from 6 GHz to more than 20 GHz. The small deviations between the simulated and measured results may were caused by the connectors and manufacturing errors. The performance of this novel LPF is experimentally characterized and evaluated with its simulation results which show a good agreement.

The proposed LPF with two DGSs in the metallic ground plane and three open stubs on the top layer with small in size of $25 \times 11 \text{ mm}^2$ is fabricated as shown in Figure 12. Figure 13 shows the measured and the simulated results. It is observed from Figure 13 that the measured results agree with the simulated one. Inspecting the measured results, the fabricated ultra wide reject band-LPF has a 3-dB cutoff frequency at 3.1 GHz, the insertion loss is as low as 0.1 dB in the passband of the filter and stopband is suppressed below -20 dB from 4 GHz to more than 20 GHz.

The performance of the proposed DGS LPF is summarized in Table 5 with other DGS LPFs for comparison. It can be seen from Table 5 that the proposed filter provides good performances in stopband rejection and passband insertion loss and more compact in size ($25 \times 11 \text{ mm}^2$) than those reported in literature [12]-[15].

VII. CONCLUSIONS

In this study, an ultra-wide reject band compact low-pass filter (LPF) using a quasi triangular of defected ground structure (DGS) along with Open Circuit Stubs has been introduced and investigated. It has been shown that the proposed DGS-LPF has achieved a return loss throughout passband range above 20 dB whereas an insertion loss in the stopband is more than 20 dB. Moreover, an ultra-wide stopband performance from 4 GHz to more than 20 GHz is also obtained. A comparison between circuit model, EM simulations and measurement results confirms the validity of the LPF configuration and the design procedure. The proposed LPF can be widely used for wideband microwave applications.

VIII. REFERENCES

- [1] D. Ahn, J. S. Park, C. S. Kim, Y. Qian, and T. Itoh, A Design of the low-pass filter using the novel microstrip defected ground structure, *IEEE Trans Microwave Theory Tech* 49 (2001), 86-91.
- [2] A. B. Abdel-Rahman, A. Verma, A. Boutejdar, and A. S. Omar, Control of bandstop response of hi-lo microstrip low-pass filter using slot in ground plane, *IEEE Trans Microwave Theory Tech* 52 (2004), 1008–1013.
- [3] J. S. Lim, C. S. Kim, D. Ahn, Y. C. Jeong, and S. Nam, Design of the low-pass filters using defected ground structure, *IEEE Trans Microwave Theory Tech* 53 (2005), 539–2545.
- [4] F. Wei, X. Shi, B. Li, Q. Huang, and X. Wang, Design of a compact microstrip low-pass filter using defected ground structure, *Microwave Opt Technol Lett* 50 (2008), 3157- 3160.
- [5] L. Lim, J. S. Park, J. S. Lee, D. Ahn, and S. Nam, Application of defected ground structure in reducing the size of amplifiers, *IEEE Microwave Guided Wave Lett* 12 (2002), 261–263.
- [6] J. P. Thakur and P. Jun-Seok, A new design approach for circular polarize antenna with DGS under the unbalanced feed-lines, *Proc. 36th European Microwave Conference, Manchester, UK, September 2006.*

- [7] J. J. Koo, S. M. Oh and M. S. Hwang, A new DGS unequal power divider, Proc. 37th European Microwave Conference, 556-559, October 2007.
- [8] H. J. Choi, J. S. Lim and Y. C. Jeong, Doherty amplifier using load modulation and phase compensation DGS microstrip line, Proc. 36th European Microwave Conference, Manchester, UK, September 2006.
- [9] Y. T. Lee, J. S. Lim, J. S. Park, D. S. Nam, A novel phase noise reduction technique in oscillators using defected ground structure, IEEE Microwave Guided Wave Lett 12 (2002), 39–41.
- [10] X. Chen, L. Wang, L. Weng and X. Shi, Compact low pass filter using novel elliptic shape DGS, Microwave Opt Technol Lett 51 (2009), 1088-1091.
- [11] S. K. Parui, S. Das, An asymmetric defected ground structure for implementation of elliptic filters, AEU International Journal of Electronics and Communications 63 (2009), 483–390.
- [12] H. J. Chen, T. H. Huang, C. S. Chang, L. S. Chen, N. F. Wang, Y. H. Wang, M. P. Houg, A novel cross-shaped DGS applied to design ultra-wide stopband low-pass filters, IEEE Microwave Wireless Comp. Lett 16 (2006), 252–254.
- [13] S. W. Ting, K. W. Tam, and R. P. Martins, Miniaturized microstrip lowpass filter with wide stopband using double equilateral u-shaped defected ground structure, IEEE Microwave Wireless Comp. Lett 12 (2008), pp. 240–242.
- [14] P. Y. Hsiao, R. M. Weng, An ultra-wide stopband low-pass filter using dual reverse U-shaped DGS, Microwave Opt Technol Lett 50 (2008), 2783-2780.
- [15] M. Al Sharkawy, A. Boutejdar, D. El Aziz and E. Galal, Design of compact microstrip filter with large reject band using a new multisectioned T-shaped defected ground structure and multilayer technique, Microw. and Optical Technology Lett 53 (2011), 1770-1774.
- [16] D. M. Pozar, Microwave Engineering, 3rd edition, John Wiley & Sons, Inc. 2005.

Table captions

TABLE 1: CHARACTERISTICS OF THE PROPOSED DGS PATTERN WITH DIFFERENT ℓ_1 ($\ell_2 = 4.84 \text{ mm}$, $g = 0.5 \text{ mm}$ AND $c = 0.94 \text{ mm}$)

TABLE 2: CHARACTERISTICS OF THE PROPOSED DGS PATTERN WITH DIFFERENT ℓ_2 ($\ell_1 = 7.14 \text{ mm}$, $g = 0.5 \text{ mm}$ AND $c = 0.94 \text{ mm}$).

TABLE 3: CHARACTERISTICS OF THE PROPOSED DGS PATTERN WITH DIFFERENT c ($\ell_1 = 7.14 \text{ mm}$, $\ell_2 = 4.84 \text{ mm}$ AND $g = 0.5 \text{ mm}$).

TABLE 4: CHARACTERISTICS OF THE PROPOSED DGS PATTERN WITH DIFFERENT g ($\ell_1 = 7.14 \text{ mm}$, $\ell_2 = 4.84 \text{ mm}$ AND $c = 0.94 \text{ mm}$).

TABLE 5: PERFORMANCE COMPARISON OF MICROSTRIP LPFS

Figure captions

Figure 1: Geometry of the proposed DGS pattern and its circuit model

Figure 2: Magnitude of S_{21} and S_{11} of the proposed DGS unit: Circuit model and Full-wave EM simulations.

Figure 3: EM field distribution results (a) in the pass band at 1 GHz, and (b) in the reject band at 5.5 GHz.

Figure 4: Magnitude of S_{21} and S_{11} of the proposed DGS for different ℓ_1 ($\ell_2 = 4.84 \text{ mm}$, $g = 0.5 \text{ mm}$ and $c = 0.94 \text{ mm}$).

Figure 5: Geometry of the proposed DGS-LPF and its circuit model

Figure 6: Simulated results of the proposed LPF using one DGS pattern and two open stubs : Full-wave EM and circuit model simulations.

Figure 7: Proposed LPF using two DGS units and three open stubs (a) Geometry, and (b) Circuit model

Figure 8: Magnitude of S_{21} and S_{11} of the proposed DGS-LPF: 01 DGS along with two open stubs and two DGSs along with three open stubs

Figure 9: Magnitude of S_{21} and S_{11} of the proposed LPF based on two DGSs and three open stubs: Full-wave EM and circuit model simulations.

Figure 10: Photography of the proposed ultra-wide reject band LPF with one DGS pattern

Figure 11: Measured and simulated S -parameters of the proposed LPF with one DGS pattern

Figure 12: Photography of the proposed ultra-wide reject band-LPF with two DGS patterns

Figure 13: Measured and simulated S -parameters of the proposed ultra-wide reject band LPF with two DGS patterns

TABLE 1

ℓ_1 (mm)	f_0 (GHz)	f_c (GHz)	S_{21max} (dB)	BW_{20dB} ^B (GHz)	L (nH)	C (pF)	R (k Ω)
5.65	7.10	4.55	-26.44	0.45	2.06	0.24	02.26
7.14	5.60	3.65	-26.46	0.43	2.73	0.32	02.31
8.48	4.70	3.05	-27.01	0.39	3.02	0.37	05.35
9.90	4.05	2.65	-27.09	0.36	3.43	0.44	05.82

TABLE 2

ℓ_2 (mm)	f_0 (GHz)	f_c (GHz)	S_{21max} (dB)	BW_{20d}^B (GHz)	L (nH)	C (pF)	R (k Ω)
3.00	6.50	4.25	-23.26	0.45	2.14	0.27	01.08
4.84	5.60	3.65	-26.46	0.43	2.73	0.32	02.31
5.00	5.25	3.55	-29.35	0.39	2.43	0.37	04.32
6.00	4.60	3.20	-32.25	0.35	2.56	0.46	08.41

TABLE 3

c (mm)	f_0 (GHz)	f_c (GHz)	S_{21max} (dB)	BW_{20dB} (GHz)	L (nH)	C (pF)	R (k Ω)
0	5.90	3.85	-26.48	0.43	2.37	0.30	02.46
1	5.60	3.65	-26.46	0.43	2.50	0.32	02.36
2	5.30	3.45	-26.43	0.43	2.65	0.33	02.21
3	5.10	3.30	-26.36	0.43	2.80	0.34	02.18

TABLE 4

g (mm)	f_0 (GHz)	f_c (GHz)	S_{21max} (dB)	BW_{20d}^B (GHz)	L (nH)	C (pF)	R (k Ω)
0.1	4.70	3.65	-28.38	0.32	0.66	1.73	03.46
0.3	5.30	3.65	-27.70	0.39	2.29	0.39	02.96
0.5	5.60	3.65	-26.46	0.43	2.50	0.32	02.23
0.7	5.80	3.65	-26.50	0.50	2.63	0.28	02.25

TABLE 5

Characteristics	[12] 2006	[13] 2006	[14] 2008	[15] 2011	This work
Substrate material (ϵ_r/h)	4.4 / 0.8	3.38 / 1.524	4.4 / 0.8	2.2 / 0.788	3.63 / 0.254
Cutoff frequency f_c (GHz)	3.5	2.4	3.7	1.37	3.1
Stopband (dB) with -20 dB rejection	4.3 - 15.8	3.26-10	3.75 - 20	4-12	4 to more than 20
Passband insertion loss (dB)	< 2	< 2.26	< 1	-	0.1
Passband return loss (dB)	-	> 5	-	> 20	> 20
Size(mm ²)	21 x 20	71 x 13	27 x 23	34 x 11	25 x 11

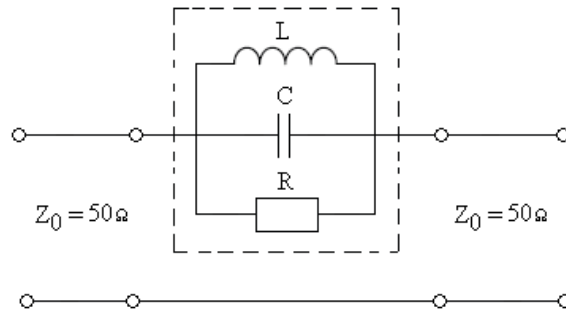
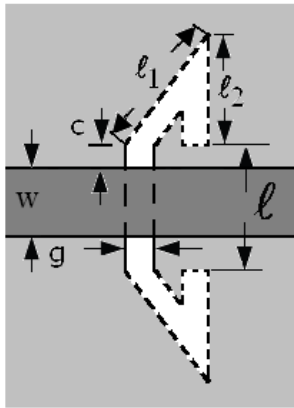


Figure 1

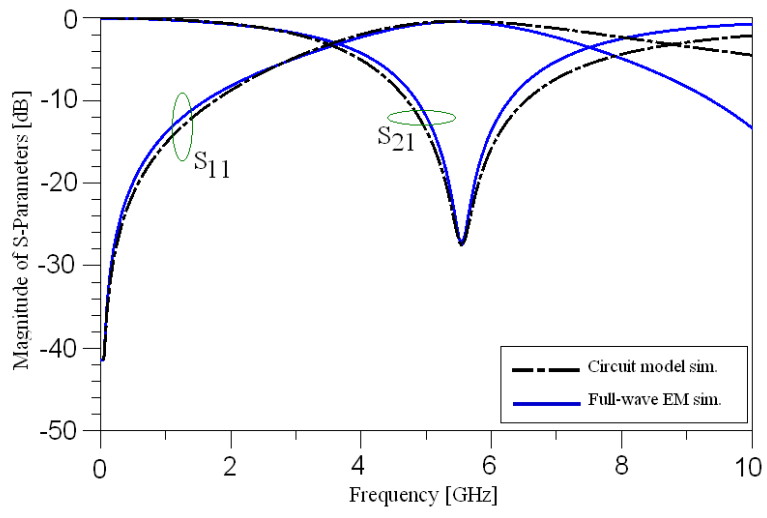
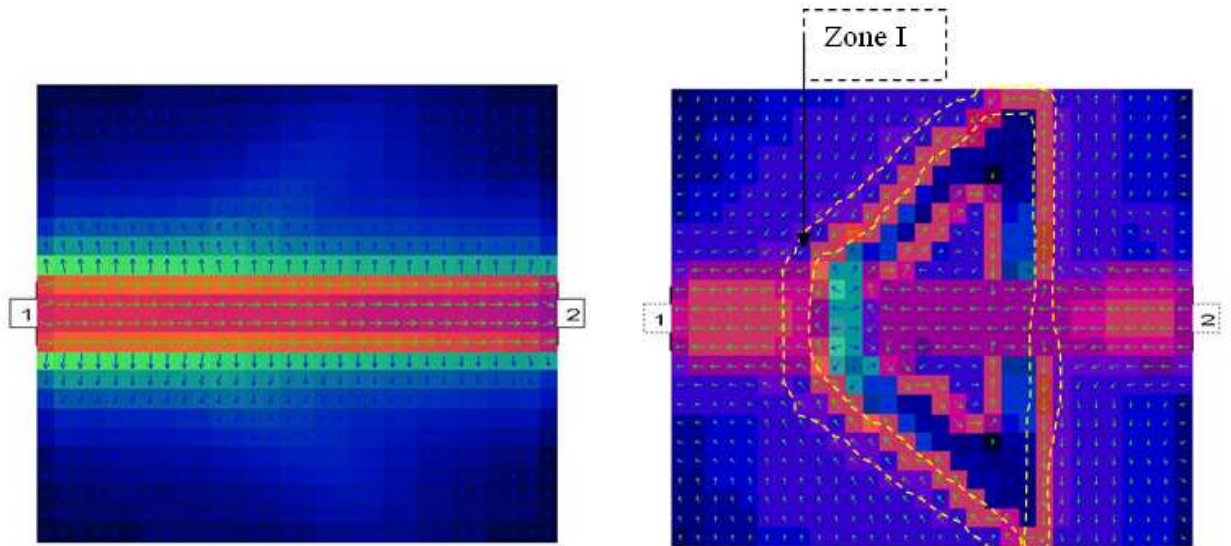
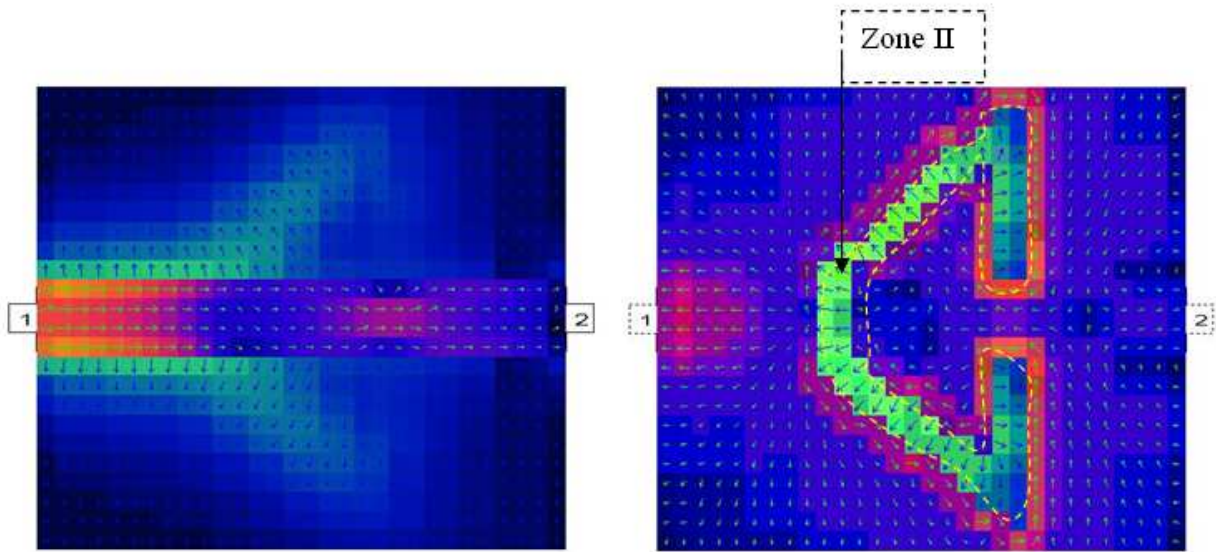


Figure 2



(a)



(b)

Figure 3

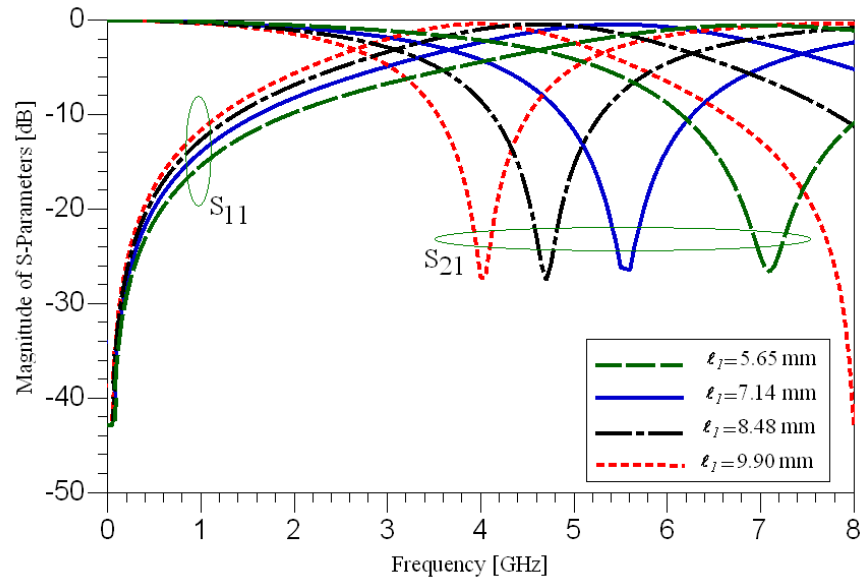


Figure 4

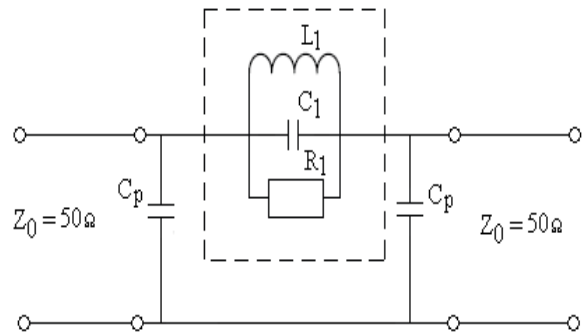
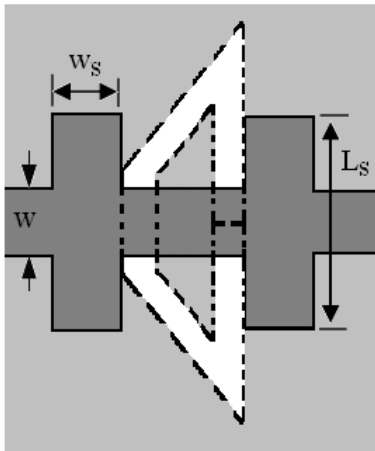


Figure 5

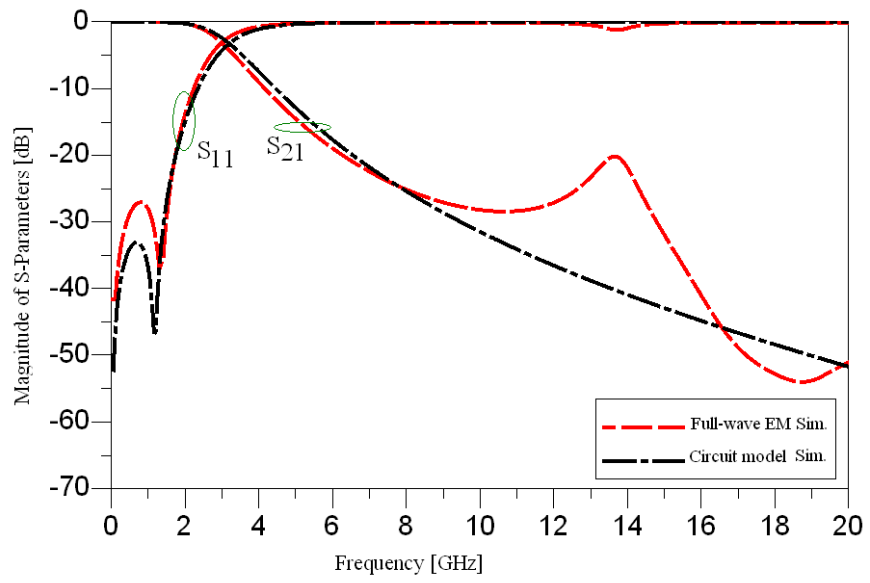
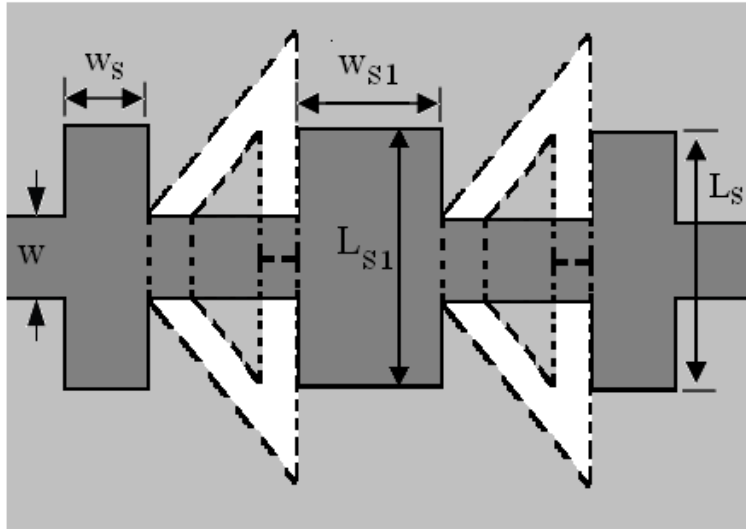
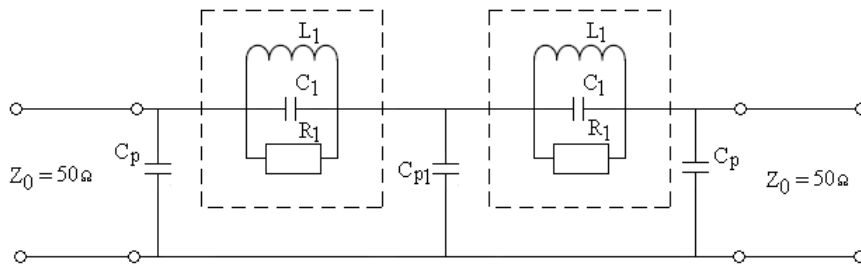


Figure 6



(a)



(b)

Figure 7

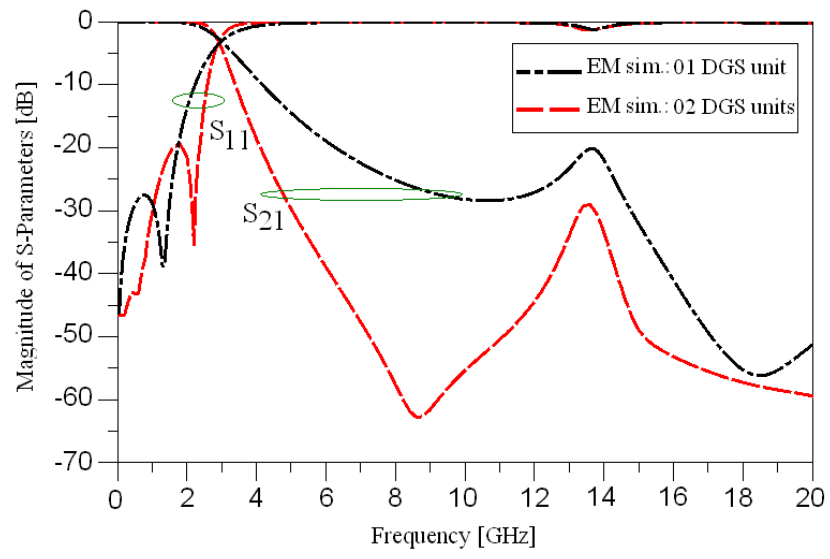


Figure 8

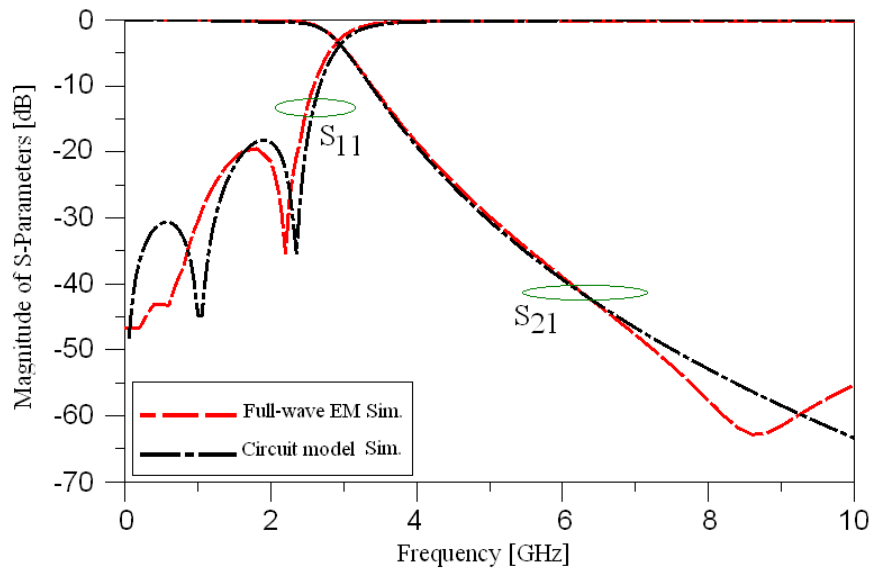


Figure 9

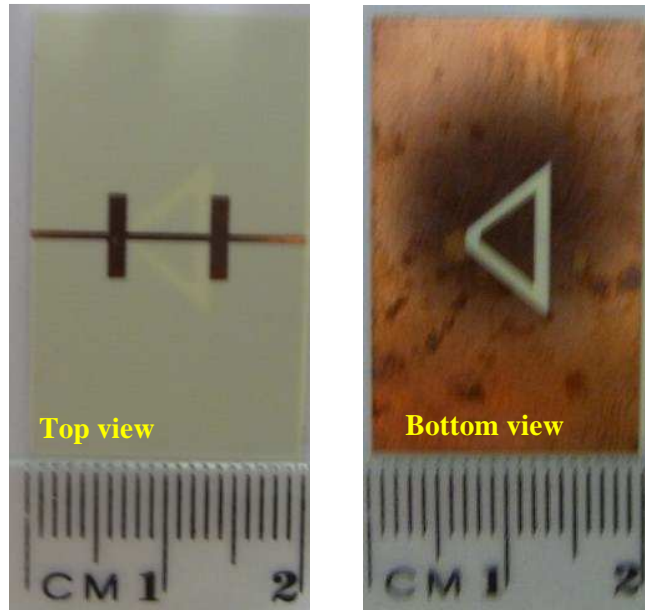


Figure 10

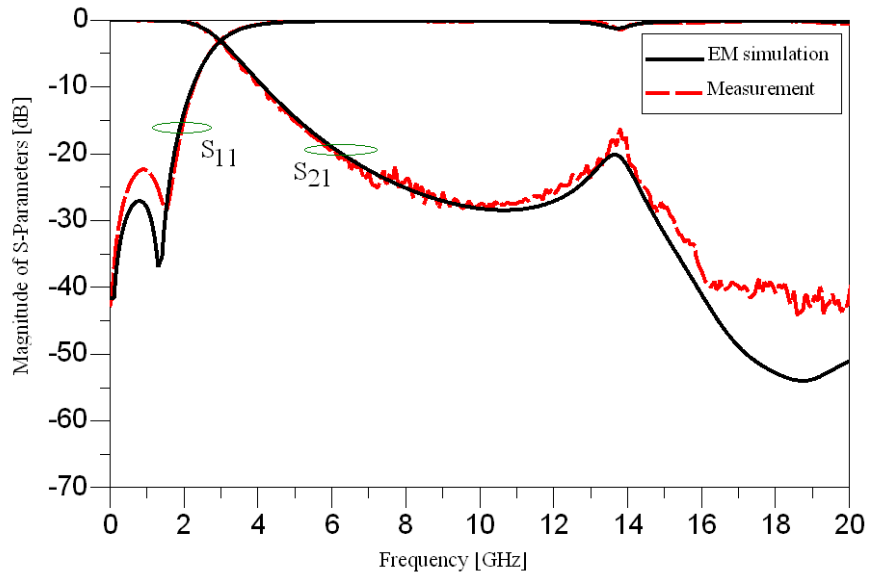


Figure 11

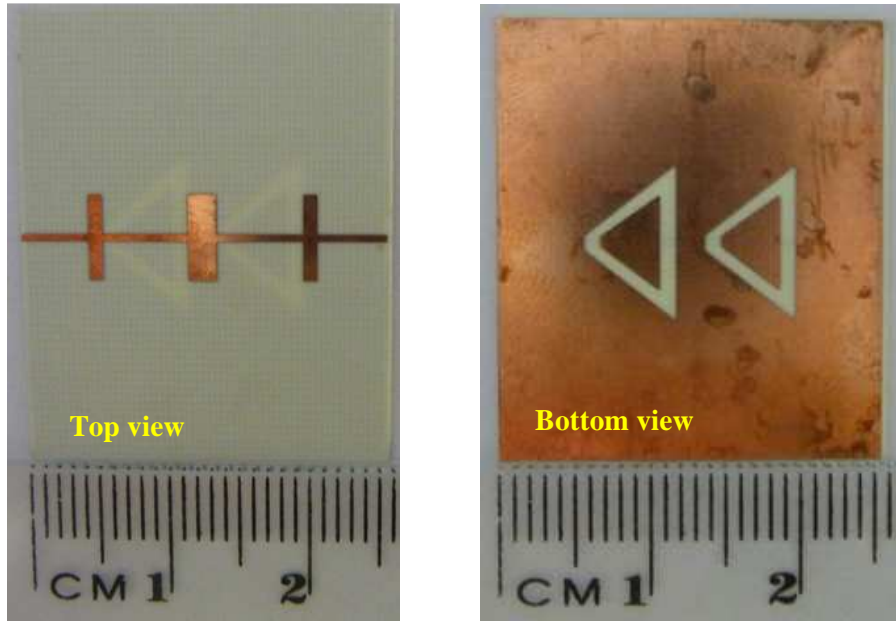


Figure 12

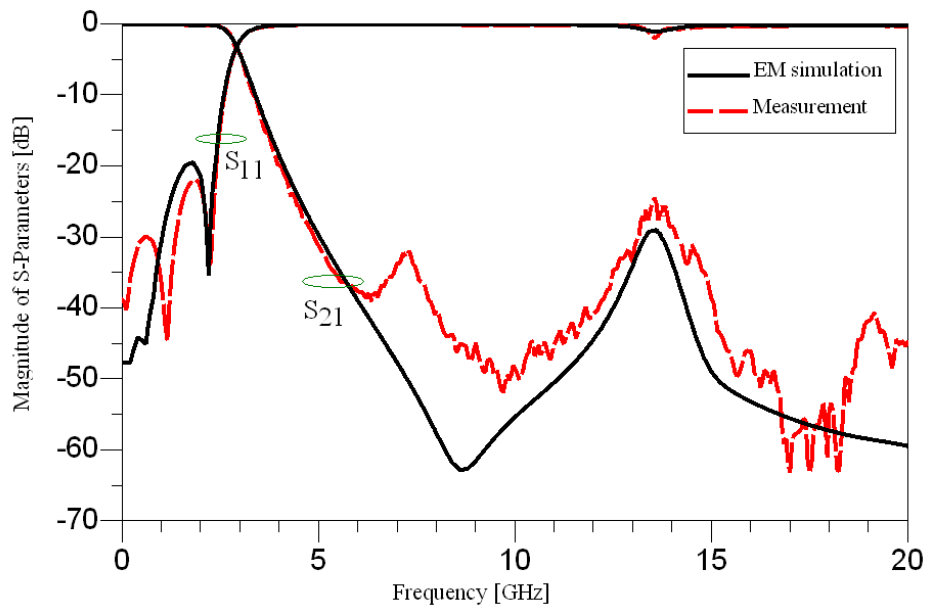


Figure 13